Free-volume Hole Properties of Two Kinds Thermoplastic Nanocomposites Based on Polymer Blends Probed by Positron Annihilation Lifetime Spectroscopy

Zhengping Fang, Yuzhen Xu, Lifang Tong

Institute of Polymer Composites, Zhejiang University, Hangzhou 310027, People's Republic of China

Received 29 December 2005; accepted 16 March 2006
DOI 10.1002/app.24569
Published online in Wiley InterScience (www.interscience.wiley.com).

ABSTRACT: Two type of nanocomposites—an immiscible blend, high density polyethylene/polyamide 6 (HDPE/PA-6) with organomodified clay, and a compatibilized blend, high density polyethylene grafted with acrylic acid/PA-6 (PEAA/PA-6) with organomodified clay—were prepared via melt compounding. X-ray diffraction and transmission electron microscopy results revealed that the clay was intercalated and partially exfoliated. Positron annihilation lifetime spectroscopy has been utilized to investigate the free-volume hole properties of two type of nanocomposites. The results show a negative deviation of free-volume size in PEAA/PA-6 blend, and a positive deviation in HDPE/PA-6 blend, and I_3 has a greater negative deviation in compatibilized blend than in immiscible blend due to interaction between dissimilar chains. For nanocomposites based on polymer blends, in immiscible HDPE/PA-6/organomodified clay system, the variation of free-volume size with clay content is not obvious and the free-volume concentration and fraction decreased. While in the case of compatibilized PEAA/PA-6/organomodified clay nanocomposites, complicated variation of free-volume properties due to interactions between two phases and organomodified clay was observed. And the interaction parameter β shows the interactions between polymers and organomodified clay. © 2006 Wiley Periodicals, Inc. J Appl Polym Sci 102: 2463–2469, 2006

Key words: blends; clay; free-volume properties; high-density polyethylene; nanocomposites; polyamide 6

INTRODUCTION

Inorganic fillers are frequently used in polymers and polymer blends with advantages that include reduced cost, improved mechanical and thermal properties,[1,2] decreased thermal expansion coefficient,[3] and enhanced ionic conductivity.[4,5]

Although a large amount of work has already been done on many aspects of polymer-layered nanocomposites during the past decade, a lot of fundamental questions still remain unanswered and need to be solved to construct the complex structure–property relationship for different nanocomposites.[6] Among the questions, an important and interesting issue is how nanodispersed layered silicate affects the motion of macromolecules located in the interfacial region, which exerts large effects on the macro properties of the composites.[7]

Many physical and chemical properties of polymers are related to their free-volume. In recent years, PALS has emerged as a unique and potent probe for characterizing the free-volume properties of polymers.[8] The unique sensitivity of PALS is due to the fact that the positronium (Ps) atoms are preferentially localized and annihilated in the free-volume holes in the amorphous regions of the polymers. PALS can be used to determine the sizes, fractions, and concentrations of free-volume holes.[9]

Many PALS measurements have been carried out to characterize the effect of filler on the free-volume of polymers. such as a PA-6/montmorillonite (MMT) nanocomposites,[10,11] polystyrene (PS)/MMT composites,[12] high-density polyethylene (HDPE)/$CaCO_3$ blend,[13] HDPE/carbon black blend,[14] and rubber-filled with carbon black.[15] And in polymer blends, some PALS results have been reported.[16–20] Hu et al.[21] studied the free-volume properties of high-impact polystyrene (HIPS)/polypropylene (PP) and HIPS/HDPE blends by means of PALS, and found that the free-volume holes in the semicrystalline polymers were not large enough to accommodate the branched chains and the end groups of the macromolecular chains in HIPS to produce favorable interactions between the semicrystalline polymers and the HIPS polymer in these blends; thus immiscible blends were formed. The weak interaction between two dissimilar polymer molecules only took place in the regions between amorphous phases.

In this paper, we report a PALS study for two well-known polymer blends with organomodified clay: a

Correspondence to: Z. Fang (zpfang@zju.edu.cn).

compatibilized blend, PEAA/PA-6 with organomodified clay, and an immiscible blend, HDPE/PA-6 with organomodified clay. The morphology of two kinds of nanocomposites and the interfacial interaction in terms of free-volume properties were investigated.

EXPERIMENTAL

Materials

The organomodified clay (C18-bentonite) was supplied by Zhejiang Huate Clay Products of China, which was ion-exchanged with octadecyl trimethyl ammonium. High-density polyethylene (HDPE, 5502#, MFR = 0.35 g/10 min) was from Daelim Corp., Korea. Polyamide 6 (PA-6, CM1017#) was from Taray Industries, Inc., Japan. Acrylic acid (AA) and dicumyl peroxide (DCP) were used as the grafting monomer and a radical initiator of HDPE respectively. All chemicals were used without further purification.

Specimen preparation

PEAA[22] was prepared in our laboratory with AA content of 8.39 wt %. HDPE/PA-6 (70/30, mass ratio, similarly hereafter), HDPE/PA-6/clay (70/30/x), PEAA/PA-6 (70/30), and PEAA/PA-6/clay (70/30/x) were prepared via melt compounding at 220°C in ThermoHaake Rheomix with a screw speed of 70 rpm, and the mixing time was 10 min for each sample. The ingredients of admixing were mixed together, and put into the container of ThermoHaake Rheomix at the same time. The mixed samples were transferred to a mold and preheated at 235°C for 3 min, then pressed at 14 MPa, and successively cooled to room temperature while maintaining the pressure to obtain the composite sheets for further measurements.

Characterization

X-ray diffraction

X-ray diffraction (XRD) was used to examine the exfoliation status of clay in composites. XRD was carried out by using a Rigaku X-ray generator (Cu Kα radiation with λ = 1.54 Å) at room temperature. The diffractograms were obtained at the scattering angles from 0.5° to 30°, at a scanning rate of 6°/min.

Transmission electron microscopy

The transmission electron micrographs were obtained with a JEM-1200EX electron microscope to examine the dispersion and exfoliation status of clay in composites. The nanocomposite samples for TEM observation were ultrathin-sectioned using a microtome equipped with a diamond knife. The sections (200–300 nm in thickness) were cut from a piece of about 1×1 mm^2, and they were collected in a trough filled with water, and placed on 200 mesh copper grid.

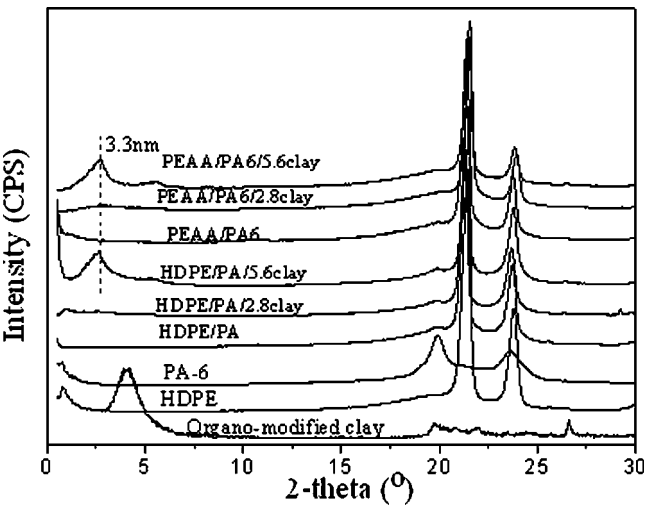

Figure 1 XRD patterns of organo-modified clay, HDPE/PA-6/organo-modified clay, and PEAA/PA-6/organo-modified clay composites.

Differential scanning calorimetry

The melting and crystallization behavior of the blend and nanocomposites were studied under nitrogen atmosphere by differential scanning calorimeter (Pyris 1), using 5–6 mg sample sealed in an aluminum pan. To avoid any effect of moisture, all the specimens were dried using vacuum oven at 80°C prior to the measurements. The temperature was raised from 50 to 250°C at a heating rate of 40°C/min, and after 3 min it was swept back at (10°C/min. Finally a heating scanning from 50 up to 250°C (at 10°C/min) was carried out.

Positron annihilation lifetime spectroscopy

A ^{22}Na positron source sealed between two aluminum foils (1 mg/cm) was sandwiched between two pieces of the same samples, which have a size of $10 \times 10 \times 1.5$ mm^3. Positron lifetime measurements were performed at room temperature by using a conventional fast-fast coincidence system that has a time resolution of 250 ps. Each spectrum contained 1×10^6 counts accumulated over a period of about 1.5 h.

In the current PAL method, the results of *o*-Ps lifetime were employed to obtain the mean free-volume hole radius by the following semiempirical equation[23]:

$$\tau_3 = \frac{1}{\lambda_3} = \frac{1}{2}\left[1 - \frac{R}{R_0} + \frac{1}{2\pi}\sin\left(\frac{2\pi R}{R_0}\right)\right]^{-1} \quad (1)$$

where τ_3 (*o*-Ps lifetime) and R (hole radius) are expressed in ns and Å, respectively. $R_0 = R + \Delta R$,

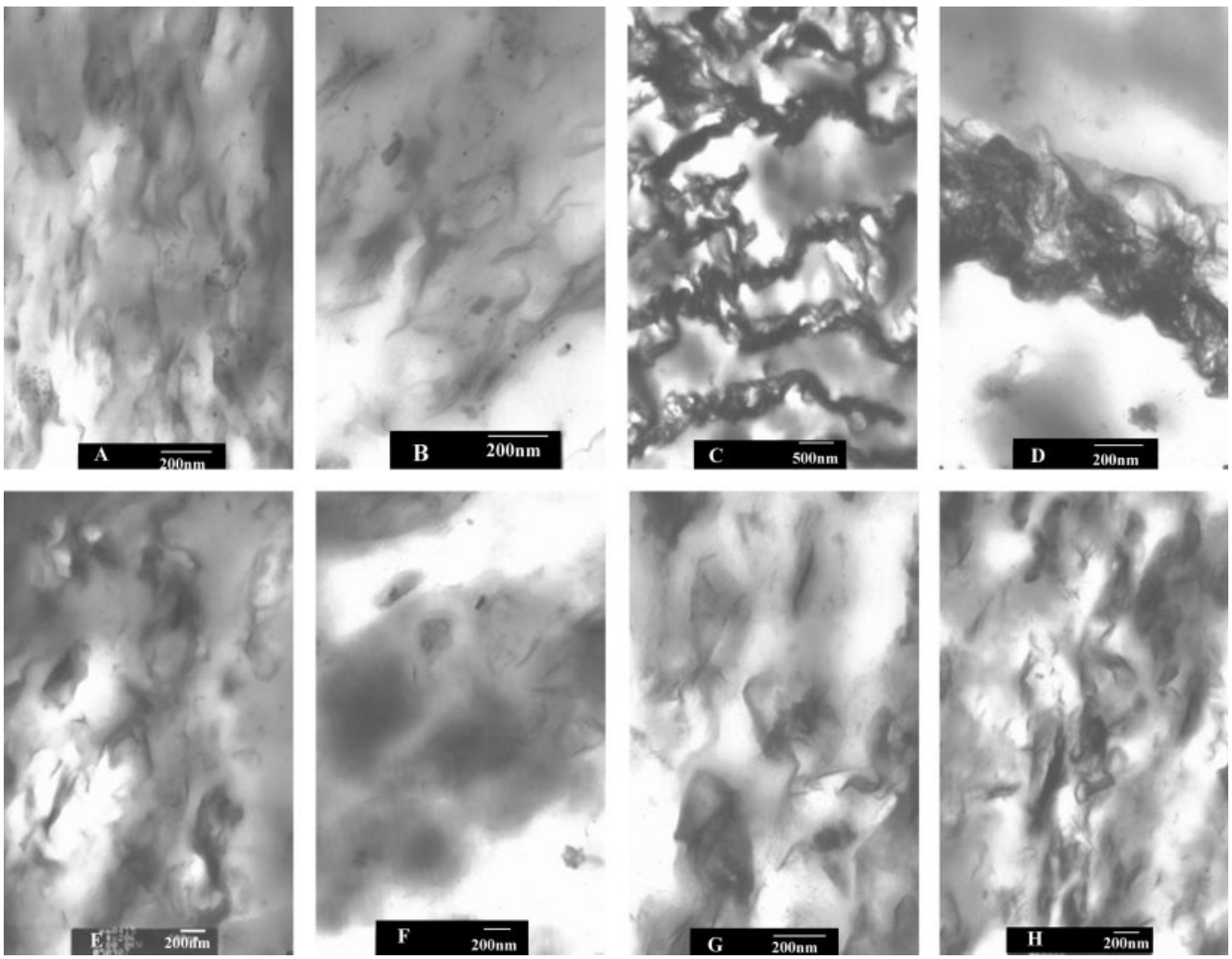

Figure 2 TEM observations for HDPE/PA-6/organo-modified clay composites containing following content of clay: (A, B) 2.8 phr, (C, D) 5.6phr; and PEAA/PA-6/organo-modified clay composites including following content of clay: (E, F) 2.8 phr, (G, H) 5.6 phr.

where ΔR is the fitted empirical electron layer thickness (= 1.66 Å).

RESULTS AND DISCUSSION

The dispersion of organomodified clay in PA-6/HDPE and PA-6/PEAA blends

To investigate the free-volume properties of the nanocomposites, we have to consider the dispersion and distribution of organomodified clay in the composites. Figure 1 shows the XRD profiles of the pure organomodified clay and its nanocomposites with HDPE/PA-6, PEAA/PA-6 blends. The (001) diffraction of the organomodified clay exhibits a broad intense peak at $2\blacksquare = 4.2^{\circ}$, corresponding to a basal spacing of 2.09 nm. For HDPE/PA-6 blend, when added 2.8 per 100 resin (phr) organomodified clay, the characteristic (001) peak of the organomodified clay shifted to a lower angle, which corresponds to spacing of 6.8–9.0 nm, indicating organomodified clay had been exfoliated. While organomodified clay content increased to 5.6 phr, the interlayer spacing reduced to 3.3 nm, corresponding to a intercalated structure. And for PEAA/PA-6 blend, XRD did not show any clay diffraction peak for PEAA/PA-6/2.8 phr organomodified clay, suggesting that the parallel stacking of the nanofiller was totally disrupted, and when 5.6 phr organomodified clay was added into PEAA/PA-6, the interlayer spacing also reduced to 3.3 nm. This may suggest that at low clay content, the clay particle mainly dispersed in PA-6 phase with exfoliated structure because of their strong interaction. When the clay content was increased, the excess clay could only be intercalated, even though the nonpolar PE was grafted with high polar AA groups.

The nanostructure of composites is illustrated in Figure 2 by TEM photography. The thin dark lines

TABLE I
Positronium Lifetime Results in HDPE/PA-6, PEAA/PA-6, and Their Composites with Organomodified Clay

Sample	Mass ratio	τ_3 (ns)	I_3 (%)	R (Å)	f_v	β
PA-6		1.5763	18.1395	2.4238	10.819	
HDPE		2.1503	22.0936	2.9822	24.547	
PEAA		2.1480	16.4096	2.9803	18.195	
HDPE/PA-6	70/30	2.0386	20.1139	2.8836	20.201	−0.0134
HDPE/PA-6/clay	70/30/2.8	2.0446	19.9113	2.8890	20.111	−0.0152
HDPE/PA-6/clay	70/30/5.6	2.0298	20.0099	2.8756	19.932	−0.0186
PA-6/PEAA	70/30	1.9736	16.8390	2.8243	15.890	−0.0845
PEAA/PA-6/clay	70/30/2.8	1.9652	16.8759	2.8164	15.793	−0.0985
PEAA/PA-6/clay	70/30/5.6	2.0336	17.5994	2.8791	17.594	−0.0637

represent the individual clay platelets, thick darker lines display stacked clay layers. The clay dispersion is agreement with that obtained from XRD results. Most of the organomodified clay is exfoliated into single platelets in HDPE/PA-6/2.8 phr organomodified clay and PEAA/PA-6/2.8 phr organomodified clay systems [Figs. 2(A), 2(B), 2(E), and 2(F)]. In Figure 2(C), the clay particles as elongated and curled areas dispersed in the PA-6 phase and gathered at interface of PA-6 and HDPE. The selective localization of the clay in the matrix is due to the difference in affinity of the organomodified clay with the two polymers. The clay layers are easily exfoliated by PA-6 molecular chains compared with HDPE molecular chains because of higher polarity of PA-6 chains. Figure 2(D) shows a higher magnification, which clearly displays the intercalation and stack of the clay. In PEAA/PA-6/5.6 phr organomodified clay system [Figs. 2(G) and 2(H)], the distribution of the clay platelets is better than that in HDPE/PA-6/5.6phr organomodified clay composite, because of higher polarity of PEAA chains, although they have same interlayer spacing.

Free-volume properties of nanocomposites

τ_3 is the annihilation lifetime of *ortho*-positronium (*o*-Ps) and has an adequate correlation with the size of intermolecular voids between polymer chains. Thus, the PALS probe sensitive to a few angstrom of intermolecular distance can provide valuable crucial information, which can be used to find correlations with the molecular level miscibility and nanoscopic phase of the blends in their solid state. The intensity of *o*-Ps lifetime, I_3, provides a measure of the relative concentration of free volume sites in the polymer unless there are strong electron-withdrawing groups that could influence trapping of *o*-Ps in the intermolecular space to the considerable extent. The measured *o*-Ps lifetimes, τ_3 and the intensities, I_3, and free-volume hole radii, R calculated according to eq. (1) of PA-6, HDPE, blends and their nanocomposites are given in Table I and Figure 3. In blends and their nanocomposites, the theoretical values of τ_3 and I_3 were obtained from the following two equations:

$$\tau_{3th} = \tau_{31}\phi_1 + \tau_{32}\phi_2 \quad (2)$$

$$I_{3th} = I_{31}\phi_1 + I_{32}\phi_2 \quad (3)$$

where τ_{3th} and I_{3th} are theoretical values of blends, τ_{31}, τ_{32}, I_{31}, and I_{32} are τ_3 and I_3 in pure polymer 1 and 2, ϕ_1 and ϕ_2 are specific volume fractions (as calculated from density and weight percent data) of component 1 and 2 polymers, respectively.

As shown in Figure 3, τ_3 of the immiscible blend HDPE/PA-6 shows a positive deviation from theoretical value, and in the case of compatibilized PEAA/PA-6 blends, free-volume was observed to decrease in size (show a negative deviation) because of intermolecular interactions, which draw molecular chains closer together. Therefore, immiscible blends may result in larger free-volume cavities because of the repulsion of different molecular chains at interfaces.

When 2.8 phr and 5.6 phr organomodified clay added into these two kind of polymer blends respec-

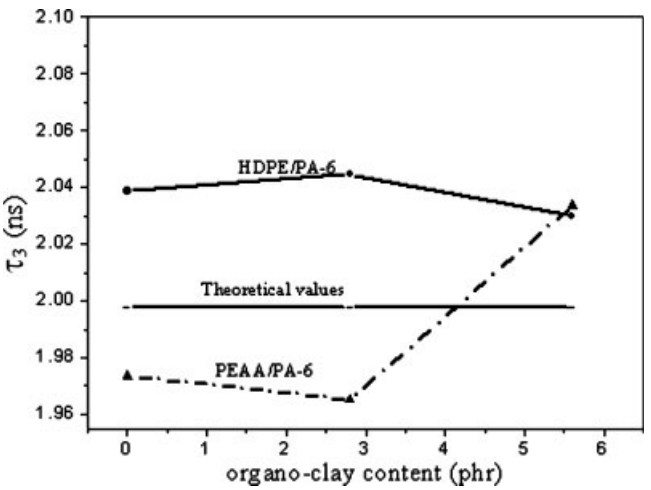

Figure 3 *o*-Ps lifetime of HDPE/PA-6 and PEAA/PA-6 blends versus clay content.

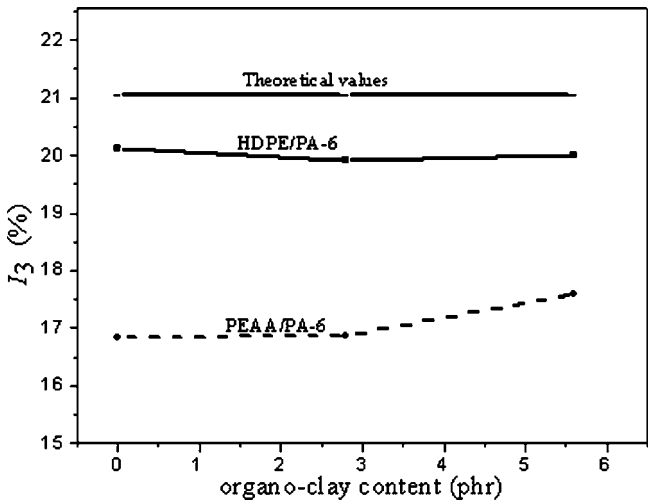

Figure 4 *o*-Ps intensities of HDPE/PA-6 and PEAA/PA-6 blends versus clay content.

tively, the variations of τ_3 as a function of organomodified clay content are different and led the following results: (1) in immiscible HDPE/PA-6 system, the variation of free-volume size is not obvious, because the clay particle had a good dispersion in PA-6 component. (2) in compatibilized PEAA/PA-6 blends, when 2.8 phr organomodified clay was added into the blends, free-volume size slightly decreased, then when more clay was added into it, the free-volume size increased.

I_3 is a measure of the number of free-volume cavities in polymers. As shown in Figure 4, I_3 has a greater negative deviation in PEAA/PA-6 blends than in HDPE/PA-6 blends, due to interactions between PEAA and PA-6 chains. In terms of interaction between dissimilar chains, a contraction of free-volume may result in a decrease of Gibb's free energy, which is a general criterion for a blend to be compatibilized. And when 2.8 phr and 5.6 phr organomodified clay was added into immiscible HDPE/PA-6 blends, the free-volume concentration slightly decreased, while in the case of compatibilized PEAA/PA-6 blend, the free-volume concentration increased.

It is because that in immiscible blends, almost all organomodified clay particles well exfoliated and dispersed in PA-6 component at low clay content, and induced in decreasing of free-volume concentration. When clay content was increased, lots of clay layers gathered at interface of PA-6 and HDPE, it can be seen from TEM results [Figs. 2(C) and 2(D)], and led to increase of I_3. And in the case of compatibilized blends, at 2.8 phr clay content, the clay platelets mainly dispersed in PA-6 matrix because of higher polarity of PA-6, and resulted in decreasing of I_3, while 5.6 phr organomodified clay was added into the blends, PEAA, a main component, easily intercalated into clay interlayers. The existence of mass intercalated structure led to increase of I_3.

Free-volume fracture ion polymers f_v can be estimated from

$$f_v = AV_f I_3 \tag{4}$$

where V_f (in Å^3) is the volume of free-volume holes calculated by using the spherical radius (R) of eq. (1) from τ_3 (in ns), I_3 (in %), and A is empirically determined to be 0.0018 from the specific volume data.

Figure 5 depicts the free-volume fraction f_v as a function of organomodified clay content, the free-volume fraction takes into account both the size and number concentration of free-volume cavities of the blends.

It is interesting to observe that the free-volume fraction is less than the fractional additive of free-volumes from two polymer components in blends. With the addition of 2.8 phr and 5.6 phr organomodified clay into HDPE/PA-6 blends, f_v decreased, while in PEAA/PA-6 blends, f_v increased with increasing clay content.

There are some free-volume theoretical interpretations concerning blending. It has been suggested that in compatibilized blends the variations of free-volume related to blending are due to the interactions between dissimilar chains and the segmental conformation and packing of component polymers for Van der waals type blends[24,25] When we consider a simple binary interchain interaction, we express the mean free-volume hole fraction f_v in a blend as[24]:

$$f_v = f_{v1}\phi_1 + f_{v2}\phi_2 + \beta f_{v1} f_{v2}\phi_1\phi_2 \tag{5}$$

where f_{v1} and f_{v2} are the free-volume hole fractions in pure polymers 1 and 2 and $\blacksquare_1$ and $\blacksquare_2$ are the specific volume fractions of polymers 1 and 2, respec-

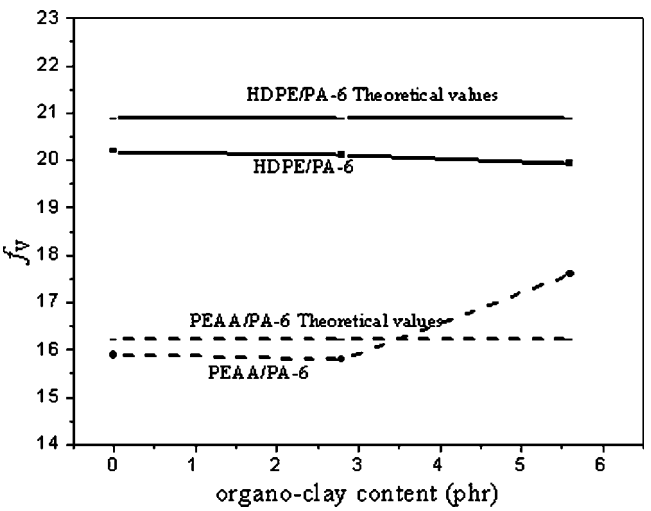

Figure 5 Free-volume fraction of HDPE/PA-6 and PEAA/PA-6 blends versus clay content.

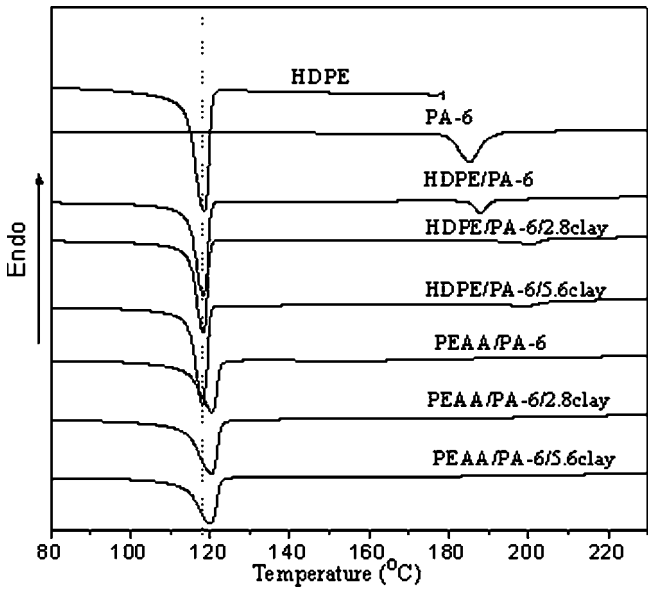

Figure 6 DSC thermograms of PA-6, HDPE, HDPE/PA-6, HDPE/PA-6/clay, and PEAA/PA-6/clay composites.

tively. Then β in eq. (5) is a parameter that could be related to the interaction between dissimilar chains. The results of β are listed in Table I.

As shown in Table I, we observe a contraction of free-volume fraction for the compatibilized PEAA/PA-6 blend ($\beta = -0.085$) and $\beta = -0.013$ for the immiscible HDPE/PA-6 blend. It is because that grafted with AA increases the polarity of HDPE chains, and improves the miscibility and interaction of HDPE and PA-6. But there is a complicated variation for the nanocomposites based on polymer blends. In immiscible blends, β was negative and decreased with increasing organomodified clay content. And in the case of PEAA/PA-6 blends, β decreased at 2.8 phr organomodified clay content, and when more organomodified clay was added into the blend, β increased to −0.064. The complicated variation of free-volume hole fractions in nanocomposites observed by the PALS is a result of the high sensitivity of the *o*-Ps atom not only to free-volume holes but also to any interfacial spaces, such as those created between boundaries of two phases and between clay platelets and polymers.

The results from PALS may not necessarily be the same as those from macroscopic measurement. Since the *o*-Ps atom probes are more appropriate for understanding interactions at the molecular level. In terms of interaction between dissimilar chains, a contraction of free-volume may result in a decrease of Gibb's free energy, which is a general criterion for the blend to be compatibilized. The current results indicate that there might be a correlation between the Flory–Huggins interaction parameter (χ) and the β parameters obtained by PALS. The negative deviation of free-volume in blends can be interpreted as a result of interaction effect of clay on the boundaries of two phases and favorable interaction of segmental conformation and packing between dissimilar molecules.[26] This suggestion will be corroborated later with DSC results.

Differential scanning calorimetry

The DSC curves and data are shown in Figure 6 and Table II. To HDPE/PA-6/clay, the crystallization temperature (T_c) for HDPE component remained unaltered with the addition of HDPE, PA6 and clay. However, the T_c for PA-6 component increased with the incorporation of clay, and the enthalpies for the crystallization transitions of PA-6 are reduced. These results firmly revealed that the clay particles are mainly dispersed in the PA-6 matrix, whereas the thermal behavior of the HDPE matrix is practically unaffected by the presence of the clay. When HDPE was modified with AA and blended with PA-6, T_c for HDPE increased, and for PA-6 component, the crystal peak disappeared, indicating a strong interaction and adhesion between the PA-6 and PEAA. To PEAA/PA-6/2.8clay system, ΔH_c^a for HDPE component slightly increased than that in HDPE/PA-6, and when the clay content was increased, ΔH_c^a decreased. These results show that organomodified clay affect the crystallization ability of two components.

TABLE II
Thermal Properties of HDPE/PA-6, PEAA/PA-6, and Their Composites with Clay

		HDPE phase		PA-6 phase	
Sample	Mass ratio	T_c (°C)	ΔH_ca (J/g)	T_c (°C)	ΔH_ca (J/g)
PA-6				185.5	−63.32
HDPE		118.4	−170.7		
HDPE/PA-6	70/30	118.3	−178.0	180.0	−47.7
HDPE/PA-6/clay	70/30/2.8	118.5	−177.9	200.3	−43.1
HDPE/PA-6/clay	70/30/5.6	118.1	−187.3	212.1	−45.8
PA-6/PEAA	70/30	120.4	−174.57		
PEAA/PA-6/clay	70/30/2.8	120.3	−187.2		
PEAA/PA-6/clay	70/30/5.6	120.1	−161.6		

CONCLUSIONS

We have reported a detailed analysis of free-volume hole size fraction and distribution in two well-characterized polymer blends: compatibilized PEAA/PA-6 and immiscible HDPE/PA-6, and their nanocomposites with organomodified clay. PALS results show a negative deviation of free-volume size in PEAA/PA-6 blend, and positive deviation in HDPE/PA-6 blend. And I_3 has a greater negative deviation in compatibilized blend than in immiscible blend. It is suggested that interaction between dissimilar chains, a contraction of free-volume may result in decreasing of Gibb's free energy, which is a general criterion for a blend to be compatibilized. In nanocomposites based on polymer blends, complicated variation of free-volume hole properties was observed. In immiscible HDPE/PA-6/organomodified clay system, the variation of free-volume size with clay content is not obvious and the free-volume concentration and fraction decreased. While in the case of compatibilized PEAA/PA-6/organomodified clay nanocomposites, complicated variation of free-volume properties was observed. It is because that the existence of intercalated structure and interaction between two components and organomodified clay affect the free-volume properties.

The authors thank Prof. Bo Wang at Wuhan University and his research group for their kind assistance in PALS measurements.

References

1. Gerard, J. F. Macromol Symp 2001, 169, 339.
2. Messersmith, P. B.; Giannelis, E. P. Chem Mater 1994, 6, 1719.
3. Yano, K.; Usuki, A.; Kurauchi, T.; Kamigaito, O. J Polym Sci Part A: Polym Chem 1993, 31, 2493.
4. Vaia, R. A.; Vasudevan, S.; Krawiec, W.; Scanlon, L. G.; Giannelis, E. P. Adv Mater 1995, 7, 154.
5. Aranda, P.; Ruiz-Hitzky, E. Chem Mater 1992, 4, 1395.
6. Ray, S. S.; Okamoto, M. Prog Polym Sci 2003, 28, 1539.
7. Wang, Y. Q.; Wu, Y. P.; Zhang, H. F.; Zhang, L. Q.; Wang, B.; Wang, Z. F. Macromol Rap Commun 2004, 25, 1973.
8. Jean, Y. C. Microchem J 1990, 42, 72.
9. Dai, Y. Q.; Wang, B.; Wang, S. J.; Jiang, T.; Cheng, S. Y. Radiat Phys Chem 2003, 68, 493.
10. Utracki, L. A.; Simha, R.; Garcia-rejon, A. Macromolecules 2003, 36, 2114.
11. Maiti, P.; Okamoto, M. Macromol Mater Eng 2003, 288, 440.
12. Tanoue, S.; Utracki, L. A.; Garcia-rejon, A.; Tatibouet, J.; Cole, K. C.; Kamal, M. R. Polym Eng Sci 2004, 44, 1046.
13. Zhang, M.; Zhang, P. F.; Zhang, S. P.; Wang, B.; Wang, S. J. Radiat Phys Chem 2003, 68, 565.
14. Jia, S. J.; Zhang, Z. C.; Fan, Y. M.; Weng, H. M.; Zhang, X. F.; Hang, R. D. Eur Polym J 2002, 38, 243.
15. Wang, J. Y.; Quarles, C. A. Radiat Phys Chem 2003, 68, 527.
16. Xie, L.; Gidley, D. W.; Hristov, H. A.; Yee, A. F. J Polym Sci Part B: Polym Phys 1995, 33, 77.
17. Kluin, J. E.; Yu, Z.; Vleeshouwers, S.; McGervey, J. D.; Jamieson, A. M.; Simha, R.; Sommer, K. Macromolecules 1993, 26, 1853.
18. Gomaa, E.; Mostafa, N.; Mohsen, M.; Mohamed, M. J Polym Mater 2004, 21, 419.
19. Maria, L. C.; Ernesto, P.; Jose, M. P.; Rosario, B.; Marijka, M.; Todor, G. Macromolecules 2005, 38, 8430.
20. Dlubek, G.; Pionteck, J.; Bondarenko, V.; Pompe, G.; Taesler, Ch.; Petters, K.; Krause-Rehberg, R. Macromolecules 2002, 35, 6313.
21. Hu, Y. H.; Qi, C. Z.; Liu, W. M.; Wang, B. Y.; Zheng, H. J.; Sun, X. D.; Zheng, X. M. J Appl Polym Sci 2003, 90, 1507.
22. Xu, Y.; Fang, Z.; Tong, L. J Appl Polym Sci 2005, 96, 2429.
23. Nakanishi, H.; Wang, S. J.; Jean, Y. C. In Positron Annihilation Studies of Dluids; Sharma, S. C., Ed.; World Scientific: Singapore, 1988; p 292.
24. Wu, S. J Polym Sci Part B: Polym Phys 1987, 25, 2511.
25. Steller, R.; Zuchowska, D. J Appl Polym Sci 1991, 38, 1411.
26. Liu, J.; Jean, Y. C. Macromolecules 1995, 28, 5774.